Greek Letters

θ = dimensionless correction factor for high flux rates
λ = latent heat of vaporization at temperature T_d, J/kg
μ = viscosity, N s/m^2
ν = kinematic viscosity, m^2/s
ρ = density, kg/m^3
χ = interception parameter, d/D

Subscripts

a = dry air properties
ab = mass transfer
b = water vapor properties
d = droplet phase
exit = venturi exit conditions
f = film properties
g = gas phase
i = injection
inlet = venturi inlet conditions
j = pertaining to the jth droplet class
j^* = total number of droplet classes considered
o = surface
ov = overall
p = particle
s = spray
T = heat transfer
th = throat conditions
x = arbitrary axial position
∞ = bulk gas properties

LITERATURE CITED

Bailey, J. E. and S. F. Liang, "Gas-Liquid Spray Contactor Modeling with Applications to Flue Gas Treatment," *Ind. Eng. Chem. Proc. Des. Dev.*, **12**, 334 (1973).

Bird, R. B., W. E. Stewart, and E. N. Lightfoot, *Transport Phenomena*, John Wiley and Sons, Inc., New York (1966).

Boll, R. H., "Particle Collection and Pressure Drop in Venturi Scrubbers," *Ind. Eng. Chem. Fund.*, **12** 40 (1973).

Dickenson, D. R. and W. R. Marshall, Jr., "The Rates of Evaporation of Sprays," *AIChE J.*, **14**, 541 (1968).

Kulic, E. and E. Rhodes, "Direct Contact Condensation from Air-Steam Mixtures," *Can. J. Chem. Eng.*, **53**, 252 (1975).

Manning, W. P. and W. H. Gauvin, "Heat and Mass Transfer to Decelerating Finely Atomized Sprays," *AIChE J.*, **6**, 184 (1960).

Placek, T. D., "The Role of Heat and Mass Transfer and Related Effects in Venturi Scrubber Performance," Ph.D. Dissertation, University of Kentucky (1978).

Placek, T. D. and L. K. Peters, "A Hydrodynamic Approach to Particle Target Efficiency in the Presence of Diffusiophoresis," *J. Aerosol Sci.*, **11**, 521 (1980).

Placek, T. D. and L. K. Peters, "Analysis of Particulate Removal in Venturi Scrubbers—Effect of Operating Variables on Performance," *AIChE J.*, **28**, 31 (1981).

Ranz, W. E. and W. R. Marshall, Jr., "Evaporation from Drops," *Chem. Eng. Prog.*, **48**, 141 (1952).

Rowe, P. N., K. T. Claxton, and J. B. Lewis, "Heat and Mass Transfer from a Single Sphere in an Extensive Flowing Fluid," *Trans. Inst. Chem. Eng.*, **43**, T14 (1965).

Manuscript received August 4, 1980; revision received January 22, and accepted February 12, 1981.

Simulation of Particulate Removal in Gas-Solid Fluidized Beds

A mathematical model for simulating particulate removal in gas-solid fluidized beds is developed based on bubble assemblage concepts and particulate collection mechanisms. The importance of fluidization mechanics on the overall fluidized bed filtration performance is emphasized in the present study. Model predictions of fluidized bed filtration efficiencies are shown to compare favorably to the experimental results of various investigations. Because of the general formulation of the proposed model, it is believed to be applicable in the design of fluidized bed filtration operations.

M. H. PETERS
LIANG-SHIH FAN
and T. L. SWEENEY

Department of Chemical Engineering
The Ohio State University
Columbus, OH 43210

0001-1541-82-5052-0039-32.00

SCOPE

Previous modeling studies on particulate removal in gas-solid fluidized beds have, for the most part, concentrated on the mechanisms by which particulates are collected and have largely ignored fludized bed mechanics. Furthermore, because of the physical nature of the process, fluidization mechanics and particulate collection mechanisms are inherently connected. In the present study the complex nature of the gas-solid fluidization process is considered in conjunction with particulate collection mechanisms. This results in a more general model of a gas-solid fluidized bed filter.

CONCLUSIONS AND SIGNIFICANCE

A general mathematical model for simulating particulate removal in gas-solid fluidized beds has been developed. By comparison with experimental results, it was found that the inclusion of fluidization mechanics as well as particulate collection mechanisms was important in the modelling of fluidized bed filters. By considering both triboelectrification and gas by-passing effects, model predictions compare well to the experimental results of various investigations. Furthermore, the

present model is believed to be the first which enables an accurate quantification of the effects of gas by-passing on overall fluid bed filter performance. Because of the general formulation of the present model it is believed to be applicable in the design of fluidized bed filters, which includes determining the effects of superficial gas velocity, particulate diameter, bed height distributor type, and a distribution of particle sizes entering the fluidized bed.

INTRODUCTION

Particulate removal in gas-solid fluidized beds has stimulated much interest due to the many operational advantages offered by the fluidized state. In this application, the fluidized bed functions as a filter to remove dusts or aerosols from a gas stream. The particle size of interest commonly ranges from 0.01 to 10 microns in diameter. Experimental investigations have shown that fluidized bed filters demonstrate a wide range of operational efficiencies (Peters, 1979). From a design standpoint, it is of interest to characterize the effects of pertinent fluid bed filtration parameters on overall performance. In general, the modeling of a fluidized bed filter is two-fold. First of all, modeling of the mechanisms by which a particle is collected, for example, inertial impaction, interception and Brownian diffusion. Secondly, modeling the complicated mechanics or hydrodynamic behavior of the gas-solid fluidization process, for example, the popular two phase models. Note here that one must distinguish between the particulates as being those aerosols or solids which are to be removed from the gas stream, and the collectors, which are the actual fluidization medium solids.

In general, the importance of mechanics or hydrodynamics on the overall performance of fluid bed operations is well known. However, in fluid bed filtration operations, the mechanics of the process plays an additional role, i.e., through determination of the actual rates of disappearance of particulates. For example, the rate of particulate collection by inertial impaction is directly dependent on the approach velocity of the particulate, which in the fluidization process, depends on the exact quantitative division of gas flow among the phases, namely, bubble, cloud and emulsion gas phase velocities. This approach greatly differs from reactant studies in gas-solid fluidized beds where information regarding the rates of disappearance or generation of a particular chemical species may be obtained independently of the fluidization process. The problem of predicting the performance of fluid bed filters is further compounded by the fact that: (1) many aspects of the collection mechanism theory have yet to be resolved (Gutfinger and Tardos, 1979); and (2) great difficulty is encountered in reproducing experimental data in identical fluid bed filtration systems (McCarthy et al., 1976). Previous modeling studies on fluid bed filtration have been largely confined to the mechanisms by which particulates are collected and have, for the most part, ignored the complicated nature of the gas-solid fluidization process (Tardos et al., 1974, Tardos et al., 1976, and Gutfinger and Tardos, 1979). Few studies have been made considering both collection mechanisms as well as fluidized bed mechanics. Doganoglu et al. (1978) have applied the two phase theory of Toomey and Johnstone (1952) in their analysis of fluid bed filtration efficiencies at superficial gas velocities far above the minimum fluidization velocity. Their analysis involves determination of a fractional jet penetration and a first order collection rate constant. However, no quantitative correlation is given for either of these two adjustable parameters. Other modeling studies recognizing both fluidization mechanics and collection efficiencies have been solely confined to electro-fluidized beds (EFB's) (Zahedi and Melcher, 1976 and 1977).

It is the objective of this paper to develop a more general mathematical model of a fluidized bed filter to provide greater insight in the design of such units. Because of its past disregard, this paper will emphasize the importance of the mechanics of the fluidization process under a simplification of particulate collection mechanisms. However, the interface between fluidization mechanics and particulate collection mechanisms will be shown, so that more sophisticated treatments to the collection mechanisms problem can be easily introduced. The conceptual model presented here for quantitatively describing the mechanics of the fluidization process is actually a simplified version of a more complex scheme, recently proposed by Peters et al. (1980), largely based on bubble assemblage concepts. Before proceeding with the model presentation, a brief review of bubble assemblage concepts is presented below.

BRIEF BACKGROUND ON BUBBLE ASSEMBLAGE CONCEPTS

The bubble assemblage concepts used in the present model are analogous to those used in the Bubble Assemblage Model proposed by Kato and Wen (1969). The Bubble Assemblage model considers an aggregative fluidized bed to be mathematically represented by a compartments-in-series type model. Each compartment is considered to be composed of two phases: a bubble phase and an emulsion phase. The height of each compartment is based on the diameter of each bubble at the corresponding bed height. It is assumed that the gas is perfectly mixed within each phase of a compartment. Therefore, the gas composition leaving a compartment is identical with that of the compartment, and any rates of disappearance or generation of a particular species are evaluated at compartment outlet conditions. The main features which will distinguish the present model from the Bubble Assemblage Model are:

(i) The inclusion of three separate phases (bubble, cloud, and emulsion phases)
(ii) The physical process of removing particulates

In addition, major two phase theory assumptions which are commonly employed in the modeling of a fluidized bed are excluded in the present model.

MODEL

The general material balance equation for the particulate removal process, assuming steady-state conditions, may be written

$$\text{Input} - \text{Output} = \text{Disappearance} \tag{1}$$

The input and output terms represent the total rate of particulates entering and leaving a given region, respectively. The disappearance term represents the total rate at which particulates are collected in the region. Figure 1a shows the schematic diagram of the model as well as the notation employed and Figure 1b shows the compartments representation. Applying Eq. 1 to the nth compartment results in the equation

$$U_{ts}S(C_{i_{n-1}} - C_{i_n}) + F_{i(i+1)_n}V_{1_n}(C_{i+1_n} - C_{i_n}) + F_{(i-1)i_n}V_{1_n}(C_{i-1_n} - C_{i_n}) = \eta_{i_n}C_{i_n}U_{ts}\frac{3(1-\epsilon_i)V_{i_n}}{2D_c} \tag{2}$$

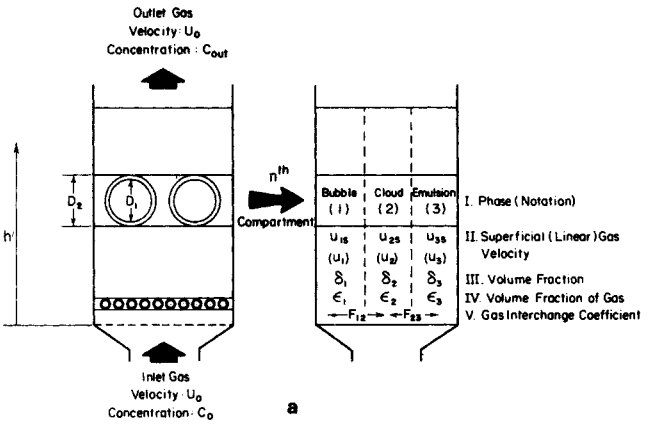

Figure 1a. Three phase transformation and phase notation of the proposed model.

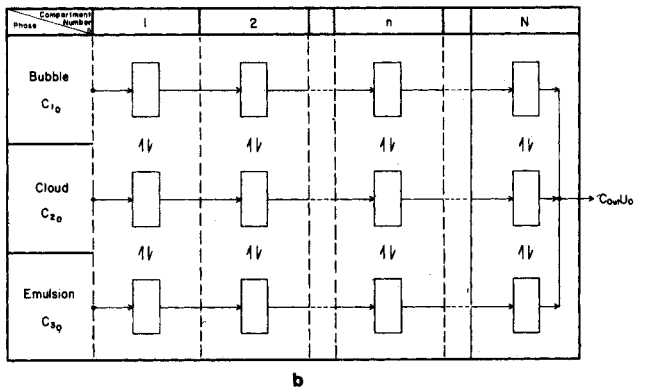

Figure 1b. Compartments representation of the proposed model.

where, $i = 1$ for the bubble phase, $i = 2$ for the cloud phase, and $i = 3$ for the emulsion phase.

Note from the term on the right-hand side of Eq. 2 that a first order rate equation for particulate collection is assumed (Doganoglu et al., 1978). Also note that the inlet gas corresponds to the zeroth compartment, thus,

$$\begin{aligned} C_{1_o} &= C_o \\ C_{2_o} &= C_o \\ C_{3_o} &= C_o \end{aligned} \tag{3}$$

As presented below, the parameters in the model may be estimated in terms of a relatively small number of fundamental parameters that characterize either the bubbling phenomenon, mass conservation, or particulate collection mechanisms.

A. Superficial Gas Velocity, U_o. In general, the superficial gas velocity can be expressed as:

$$U_o = U_{1s} + U_{2s} + U_{3s} \tag{4}$$

where U_{1s}, U_{2s}, and U_{3s} are constant throughout the fluidized bed.

B. Superficial Gas Velocity in the Bubble Phase, U_{1s}. The superficial gas velocity in the bubble phase is related to the average linear bubble phase gas velocity and the average bubble phase volume fraction by:

$$U_{1s} = \overline{U}_1 \bar{\delta}_1 \epsilon_1 \tag{5}$$

where $\overline{U}_1$ and $\bar{\delta}_1$ are computed from the relationships given in sections *E.* and *N.*, respectively.

C. Superficial Gas Velocity in the Cloud Phase, U_{2s}. Since a bubble and its cloud rise together at the same linear velocity, the supeficial gas velocity in the cloud phase is given by

$$U_{2s} = \frac{\bar{\delta}_2 \epsilon_2}{\bar{\delta}_1 \epsilon_1} U_{1s} \tag{6}$$

where $\bar{\delta}_2/\bar{\delta}_1$ is given in section *G.*

D. Superficial Gas Velocity in the Emulsion Phase, U_{3s}. Substituting Eqs. 5 and 6 into Eq. 4 gives the superficial gas velocity in the emulsion phase, as:

$$U_{3s} = U_o - \overline{U}_1(\bar{\delta}_1 \epsilon_1 + \bar{\delta}_2 \epsilon_2), \tag{7}$$

subject to the stipulation that

$$U_o > \overline{U}_1(\bar{\delta}_1 \epsilon_1 + \bar{\delta}_2 \epsilon_2). \tag{8}$$

E. Linear Gas Velocity in the Bubble Phase, U_1. The linear gas velocity in the bubble phase may be computed from the commonly accepted relationship proposed by Davidson and Harrison (1963).

$$U_1 = (U_o - U_{mf}) + 0.71\sqrt{GD_1} \tag{9}$$

The average linear gas velocity in the bubble phase may be expressed as:

$$\overline{U}_1 = (U_o - U_{mf}) + 0.71\sqrt{G\overline{D}_1} \tag{10}$$

F. Linear Gas Velocities in the Cloud and Emulsion Phases, U_2 and U_3. The linear gas velocities in the cloud and emulsion phases may be computed from their corresponding superficial gas velocities by,

$$U_2 = \frac{U_{2s}}{\delta_2 \epsilon_2} \tag{11}$$

$$U_3 = \frac{U_{3s}}{\delta_3 \epsilon_3} \tag{12}$$

G. Volume Ratio between Cloud and Bubble Phases, δ_2/δ_1. The volume ratio between the cloud phase and the bubble phase may be computed from the theoretical model of Davidson and Harrison (1963) as,

$$\frac{\delta_2}{\delta_1} = \frac{3U_{mf}}{\epsilon_{mf}U_1 - U_{mf}}, \tag{13a}$$

and the average volume ratio may be expressed as:

$$\frac{\bar{\delta}_2}{\bar{\delta}_1} = \frac{3U_{mf}}{\epsilon_{mf}\overline{U}_1 - U_{mf}} \tag{13b}$$

H. Bubble Diameter, D_1. A recent correlation, which considers the effects of bed diameters and distributor types, is utilized (Mori and Wen, 1975). This correlation, based on the bubble diameter data appearing in the literature prior to 1974 is:

$$\frac{D_{1_m} - D_1}{D_{1_m} - D_{1_o}} = \exp(-0.3h/D_R) \tag{14}$$

where

$$D_{1_m} = 0.652[S(U_o - U_{mf})]^{2/5} \tag{15}$$

and

$$D_{1_o} = 0.347\left[\frac{S(U_o - U_{mf})}{N_D}\right]^{2/5} \tag{16}$$

(for perforated distributor plates)

$$D_{1_o} = 0.00376(U_o - U_{mf})^2 \tag{17}$$

(for porous distributor plates)

This correlation is valid over the following variable ranges:

$$0.5 < U_{mf} < 20, \text{ cm/s}$$

$$0.006 < D_c < 0.045, \text{ cm}$$

$$U_o - U_{mf} < 48, \text{ cm/s}$$

$$D_R < 130, \text{ cm}$$

I. Gas Interchange Coefficients. Based on the Davidson model the following expressions have been derived for gas interchange coefficients between bubble and cloud phases, and for that between cloud and emulsion phases (Kunii and Levenspiel, 1968; Davidson and Harrison, 1963).

$$F_{12} = 4.5\left(\frac{U_{mf}}{D_1}\right) + 5.85\left(\frac{G^{0.25}D_G{}^{0.5}}{D_1{}^{1.25}}\right) \quad (18)$$

$$F_{23} = 6.78\left(\frac{\epsilon_{mf}D_G U_1}{D_1{}^3}\right)^{0.5} \quad (19)$$

Note that $F_{01} = F_{34} = 0$.

J. Expanded Bed Height. The height of bed expansion can be approximated as (Peters et al., 1980)

$$L = L_{mf} + \frac{YL(U_o - U_{mf})}{U_o - U_{mf} + 0.71\sqrt{G\overline{D}_1}} \quad (20)$$

where

$$\overline{D}_1 = D_{1_m} - (D_{1_m} - D_{1_o})\exp(-0.15L_{mf}/D_R), \quad (21a)$$

and

$$Y = 0.76 \quad (21b)$$

K. Volume Fraction Gas in Each Phase. The volume fraction of gas in the cloud and emulsion phases is assumed to be equal to that at minimum fluidization:

$$\epsilon_2 = \epsilon_3 = \epsilon_{mf}$$

The model assumes a value of 1.0 for the volume fraction of gas in the bubble phase.

L. Number of Bubbles in a Compartment, N. With compartment height based on the diameter of the cloud, the number of bubbles can be computed from material balance considerations as well as some assumptions concerning the average solids volume fraction in the bed (Peters et al. 1980).

$$N = \frac{6SD_{2_n}(\epsilon - \epsilon_{mf})}{\pi D_{1_n}^3(1 - \epsilon_{mf})} \quad (22)$$

where

$$1 - \epsilon = \frac{L_{mf}}{L}(1 - \epsilon_{mf}) \quad (23)$$

$$\text{for } h \le L_{mf}$$

and

$$1 - \epsilon = \frac{L_{mf}}{L}(1 - \epsilon_{mf})\left\{\exp\left[-\left(\frac{h - L_{mf}}{L - L_{mf}}\right)\right]\right\} \quad (24)$$

for $L_{mf} \le h$

M. Cloud Diameter, D_2. The diameter of the cloud may be easily obtained by rearranging Eq. 13a to give:

$$\left(\frac{D_2}{D_1}\right)^3 = \frac{\epsilon_{mf}U_1 + 2U_{mf}}{\epsilon_{mf}U_1 - U_{mf}} \quad (25a)$$

as well as the average cloud diameter as:

$$\left(\frac{\overline{D}_2}{\overline{D}_1}\right)^3 = \frac{\epsilon_{mf}\overline{U}_1 + 2U_{mf}}{\epsilon_{mf}\overline{U}_1 - U_{mf}} \quad (25b)$$

N. Volume fraction of each phase, δ_i. The volume fraction of the bubble, cloud and emulsion phases may be computed as:

$$\delta_{i_n} = V_{i_n}/SD_{2_n} \quad (26)$$

where $i = 1$ for the bubble phase, $i = 2$ for the cloud phase, $i = 3$ for the emulsion phase, and

$$V_{1_n} = N(1/6)\pi D_{1_n}^3 \quad (27)$$

$$V_{2_n} = V_{1_n}\left[\frac{3U_{mf}}{\epsilon_{mf}U_1 - U_{mf}}\right] \quad (28)$$

$$V_{3_n} = SD_{2_n} - V_{2_n} - V_{1_n} \quad (29)$$

Note that,

$$\overline{\delta}_1 = \overline{V}_1/S\overline{D}_2 \quad (30)$$

$$\text{and } \overline{V}_1 = \overline{N}(1/6)\pi\overline{D}_1{}^3 \quad (31)$$

where $\overline{N}$ is evaluated at $h = L_{mf}/2$ and $\overline{D}_1$ is given by Eq. 21a.

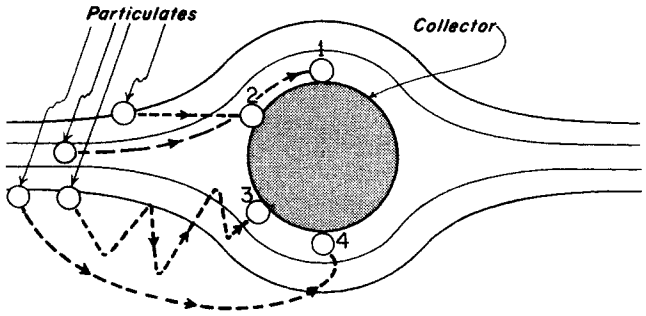

1 - Interception

2 - Impaction

3 - Brownian Motion

4 - Induced Electrostatic Forces

a

Figure 2a. Collection mechanisms considered in the proposed model.

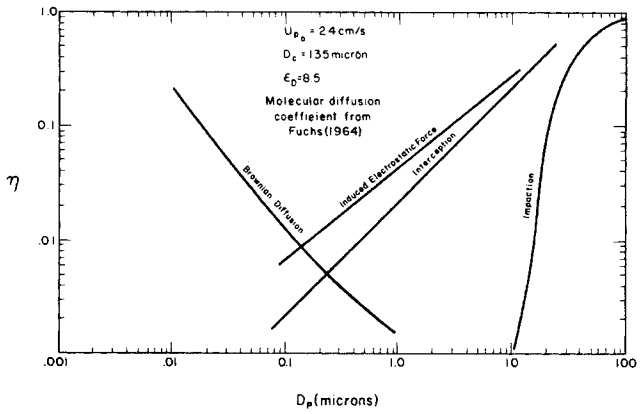

b

Figure 2b. Single spherical collector efficiencies.

O. Collector Efficiencies. Four collection mechanisms will be considered: inertial impaction, interception, Brownian movement, and induced electrostatic forces. These mechanisms are illustrated in Figure 2a. Figure 2b shows a typical plot of the single spherical collector efficiencies versus particulate diameter for the four collection mechanisms as given in the equations below.

Inertial Impaction. A particle approaching a collector may deviate from the stream lines, due to its inertia, and strike the collector. The classic analysis of Langmuir (1948) is used in this study. Impaction efficiencies are calculated from the relationship derived by assuming Stoke's law for the particle in an ideal fluid,

$$\eta_{\text{IMP}} = \frac{(\text{Stk})^2}{(\text{Stk} + 1/2)^2} \quad (32)$$

where $\text{Stk} = \frac{1}{9}\frac{D_P{}^2U_{p_o}\rho_p}{\mu D_c}$

Interception. A massless but finite size particle may pass close enough to the collector for its surface to touch. Assuming ideal flow around the collector, and that the particle will touch the collector whenever its center approaches within a distance $D_p/2$ from the surface, the efficiency of interception is given by Ranz and Wong (1952), as:

$$\eta_{\text{INT}} = (1 + N_I)^2 - \frac{1}{1 + N_I} \quad (33)$$

Brownian movement. When particle size is small, random movement may lead to collection. The analysis of Levich (1962) is used

TABLE 1. SUMMARY OF ISOLATED SINGLE SPHERICAL COLLECTOR EFFICIENCIES

COLLECTION MECHANISM	COLLECTION EFFICIENCY	REFERENCES	REMARKS
1. Inertial Impaction	$\eta_{IMP} = \frac{(Stk)^2}{(Stk + \frac{1}{2})^2}$	Langmuir (1948)	Stoke's Law for the drag force on the particle and ideal fluid flow around the collector. $(Stk)_{crit.} = 0.0833$
	$\eta_{IMP} = \left[\frac{1 + (3/4)\ (\ln 2\ Stk)}{(Stk - 1.214)}\right]^{-2}$	Langmuir (1948)	Stoke's Law for the drag force on the particle and viscous flow around the collector. $(Stk)_{crit.} = 1.214$
2. Gravity Settling	$\eta_G = \frac{U_s}{U_{p_o}}$	Ranz and Wong (1952) Chen (1955) Paretsky (1974)	
3. Electrostatic Forces	$\eta_{ELECT} = 4K_c$	Nielsen and Hill (1976)	Coulombic Force. Independent of flow field around collector.
	$\eta_{ELECT} = 1.58K_{IP}^{\frac{1}{2}}$	Nielsen and Hill (1976)	Charged Particle Image Force. Viscous Flow around collector. $(0.002 \le K_{IP} \le 0.1)$
	$\eta_{ELECT} = 2.89K_{IP}^{0.353}$	Nielsen and Hill (1976)	Charged Particle Image Force. Potential Flow around collector. $(0.002 \le K_{IP} \le 0.1)$
	$\eta_{ELECT} = (\frac{15\pi}{8} K_{IC})^{0.4}$	Kramer and Johnstone (1955)	Charged collector image force. Only an approximate result. See Nielsen and Hill (1976) for graphical presentation.
			Parameter K: Coulombic force: $K_c = \frac{CQ_pQ_{ac}}{3\rho\mu D_p U_{p_o} \epsilon_o}$ Charged-particle image force: $K_{IP} = \frac{CQ_p^2}{3\pi^2\mu D_p U_{p_o} \epsilon_o D_c^2}$ Charged-collector image force: $K_{IC} = \frac{(\epsilon - 1)8CD_p^2Q_{ac}^2}{(\epsilon + 2)3\mu D_c U_{p_o} \epsilon_o}$
4. Interception	$\eta_{INT} = (1 + N_I)^2 - \frac{1}{(1 + N_I)}$	Ranz and Wong (1952)	Ideal fluid flow around the collector.
	$\eta_{INT} = (1 + N_I)^2 - \frac{3}{2}(1 + N_I) + \frac{1}{2}(\frac{1}{1 + N_I})$	Friedlander (1957)	Viscous flow around the collector.
5. Brownian Diffusion	$\eta_{BD} = 3.988 N_{Pe}^{-2/3}$	Friedlander (1957) Levich (1962) Tardos et al (1976)	$N_{Pe} > 1000$

in the present study. For mass transfer to a single sphere falling in an infinite fluid, the result in terms of a collection efficiency is:

$$\eta_{BD} = 4.04(N_{Pe})^{-2/3} \tag{34}$$

Induced Electrostatic Collection. During the fluidization process the bed becomes electrically charged as a result of internal friction between dielectric bed medium solids (Ciborovsky and Wlodarsky, 1962). In fluid bed filtration, this triboelectrification effect can lead to particulate collection by charged collector image forces. Induced electrostatic efficiencies are calculated from the approximate equation given by Kramer and Johnstone (1955) as

$$\eta_{ELECT} = \left(\frac{15\pi}{8} K_{IC}\right)^{0.4} \tag{35}$$

where

$$K_{IC} = \frac{(\epsilon_D - 1)2CD_p^2Q_{AC}^2}{(\epsilon_D + 2)3\mu D_c U_{p_o} \epsilon_o}$$

In the absence of experimental data the value of the charge density on the dielectric bed medium solids is taken to be two order of magnitudes less than the maximum value for surfaces charged in air (Ciborows and Zakowski, 1977). The approach velocity of the particulates, U_{p_o}, used to obtain η_{IMP}, η_{BD}, and η_{ELECT} is taken to be the linear velocity of the gas in each phase, which is given by Eqs. 11 and 12. Also note from Eqs. 11 and 12 that the linear velocity of the gas is allowed to vary throughout the bed. It is assumed that the value of the single collector efficiency in any phase at a given compartment is obtained from the sum of the four mechanisms considered times a multicollector correction factor

$$\eta_i = [g(\epsilon)(\eta_{IMP} + \eta_{INT} + \eta_{BD} + \eta_{ELECT})]_i \tag{36}$$

Equations 32–35 are strictly applicable to an isolated single sphere, i.e., a single sphere situated in an infinite fluid. The correction factor appearing in Eq. 36 represents a velocity profile ratio between an isolated single sphere and a single sphere situated in a swarm of similar spheres (Tardos et al., 1976). The correction factor, which is a function of the volume fraction of gas in each phase, may be approximated as (Tardos et al., 1976):

TABLE 2. COMPUTATIONAL SEQUENCE FOR PARAMETRIC EVALUATION AT THE nth COMPARTMENT

Sequence	Eq. Number	Calculated Parameter
1	14	D_1
2	9	U_1
3	13a	δ_2/δ_1
4	23, 24	ϵ
5	22	N
6	27, 28, 29	V_1, V_2, V_3
7	26	δ_i
8	18, 19	F_{12}, F_{23}
9	11, 12	U_2, U_3
10	36	η_i

$$[g(\epsilon)]_i = \frac{1.3}{\epsilon_i} \tag{37}$$

It should be noted that the use of the isolated single collector efficiency expressions give in Eqs. 32–35, as well as the expression for the net single collector efficiency, Eq. 36, is controversial. However, their use does not deviate from the purposes of the present study. Table 1 summarizes the various literature expressions available for evaluating the isolated single spherical collector efficiencies. Note that gravity settling, charged particle image forces, and Coulombic forces have not been included in the present model. In general, the expressions given in Table 1 are highly dependent on the type of flow field assumed around the collector. Literature modifications of some expressions appearing in Table 1 to the non-isolated case have been recently reviewed by Tardos et al. (1978).

The volumetric average particulate concentration at the exit of the bed is expressed by:

$$C_{\text{out}} = C_{1_N}\frac{U_{1s}}{U_o} + C_{2_N}\frac{U_{2s}}{U_o} + C_{3_N}\frac{U_{3s}}{U_o}, \tag{38}$$

and the overall collection efficiency is defined as

$$X = 100\left(\frac{C_o - C_{\text{out}}}{C_o}\right) \tag{39}$$

It has been shown that at high superficial velocities, i.e., U_o/U_{mf} greater than approximately six to eleven, flow reversal of gas in the emulsion phase can occur (Kunii and Levenspiel, 1968). This situation is not included in the model presented here and is explicitly stated in Eq. 8. It is assumed that the equations given above describing the flow of gas in a fluidized bed are also applicable to the flow of particulates, and that the collected particulates are not re-entrained by the gas flow. For values of the superficial gas velocity close to the minimum fluidization velocity, clouds may not exist in the entire region of the fluidized bed. A straight-forward simplification of the model presented here for this situation is given in Appendix 1.

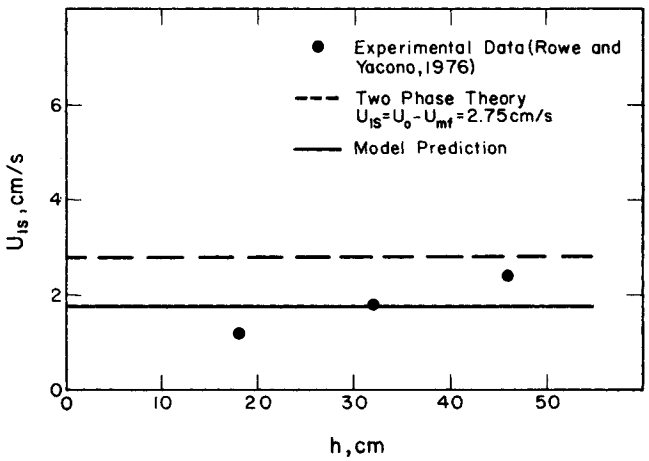

Figure 3. Superficial bubble phase gas velocity as a function of the height from the distributor. $U_o - U_{mf} = 2.75$.

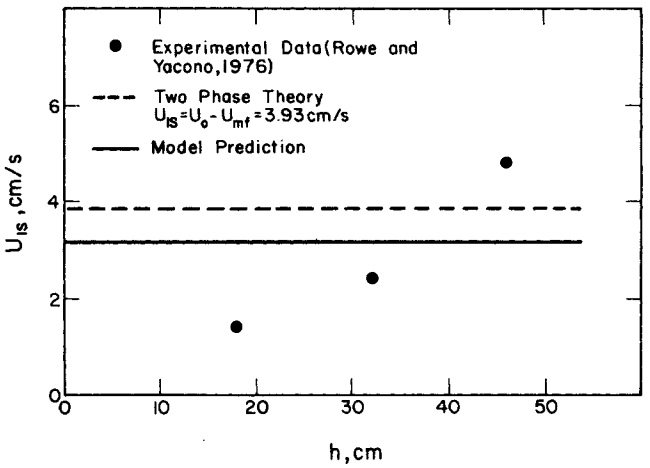

Figure 4. Superficial bubble phase gas velocity as a function of the height from the distributor. $U_o - U_{mf} = 3.93$.

METHOD OF SOLUTION

The computational procedure based on the proposed model is summarized below.

Calculations of the overall collection efficiency and concentration profiles begin with specification of the values of the superficial gas velocity, U_o, minimum fluidization velocity, U_{mf}, bed height at minimum fluidization, L_{mf}, void fraction at minimum fluidization, ϵ_{mf}, void fractions in each phase, ϵ_i, column diameter, D_R, molecular diffusion coefficient of particulate, D_G, collector diameter, D_c, density of particulate, ρ_p, particulate diameter, D_p, and the dielectric constant of particulate, ϵ_D. There are no adjustable parameters in the present model.

Because bubble diameter is a function of the height from the distributor, and the height from the distributor is taken to the center of the bubble in question, and iterative procedure is used to determine D_1. The initial guess is taken to be the bubble diameter computed for the previous compartment.

For each compartment there are three material balance equations with three unknowns, the concentrations in each phase, namely: bubble, cloud and emulsion phases. These may be solved by a matrix reduction scheme or a trial and error procedure. The average superficial gas velocities in each phase are first determined from Eqs. 5, 6 and 7. The computational sequence for the remaining parameters in Eq. 2 is given in Table 2. Calculations are carried out up to the expanded bed height, L. It is assumed here that the size of the last compartment is determined from the difference between the cumulative compartments size and the height of the expanded bed. However, for consistency, gas interchange coefficients and the linear bubble phase gas velocity are based on a hypothetical bubble diameter predicted from Eq. 14.

RESULTS AND DISCUSSION

Graphical results of the computer solution based on the present model are shown in Figures 5–11 with the input parameters given in Tables 3–5. The computational scheme given here for evaluating the superficial gas velocities in each phase is new and actually represents a simplified version of a more complex scheme recently proposed by Peters et al. (1980). A partial verification of the present method is shown in Figs. 3 and 4, where the predicted superficial bubble phase gas velocity as a function of the height from the distributor is compared to both the two phase theory and the experimental data of Rowe and Yacono (1976). Note that in these cases both the model prediction and the experimental data show that the two phase theory tends to over-predict the bubble phase flow rate. Experimental measurements of Grace and Harrison (1969), Werther (1974), and Chavarie and Grace (1975) also support the results presented in Figures 3 and 4.

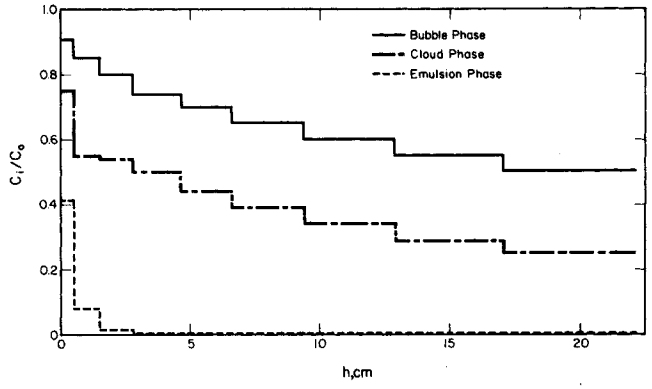

Figure 5. Particulate concentration profiles for bubble, cloud, and emulsion phases in a fluidized bed filter.

AXIAL CONCENTRATION PROFILES

Figure 5 shows a typical result predicted by the present model for the variation of particulate concentration in each phase with the height from the distributor. Several aspects of these curves are noteworthy:

(i) The majority of particulate collection in the emulsion phase occurs in a relatively short distance from the distributor.

(ii) The decrease in particulate concentration in the bubble phase is solely due to gas interchange among the phases.

(iii) The decrease in particulate concentration in the cloud phase is more rapid than the bubble phase due to both gas interchange and particulate collection.

DEPENDENCE OF THE OVERALL COLLECTION EFFICIENCY ON SUPERFICIAL GAS VELOCITY

The effect of superficial gas velocity on the overall collection efficiency is a major concern in the design of fluid bed filters. In general, superficial gas velocity affects the present model through both the fluidiziation mechanics and the collection mechanisms. Figure 6 shows a typical simulation result obtained from the present model for the dependence of the overall collection efficiency on both superficial gas velocity and particulate collection mechanism type. The general trend of decreasing overall collection efficiencies with increasing superficial gas velocity is due to gas by-passing effects, i.e., larger, and thus faster, bubbles. The relative slopes of the overall collection efficiency profiles shown in Figure 6 are directly associated with the particulate collection mechanism type. In Case I, where Brownian diffusion is the controlling mechanism, the decrease in the overall collection efficiency with increasing superficial gas velocity is greater than that for Case II or III. This

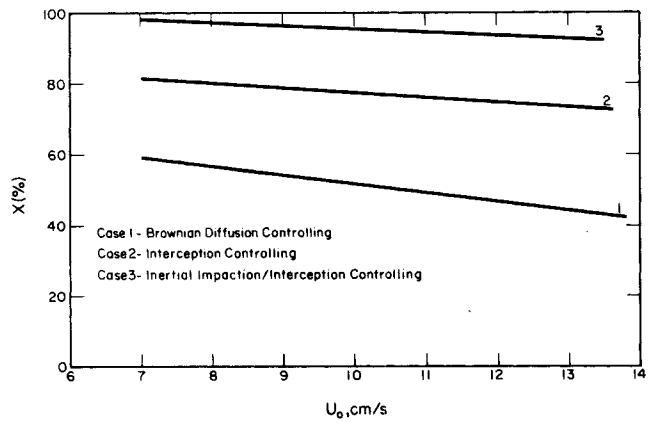

Figure 6. Dependence of the overall collection efficiency on superficial gas velocity and collection mechanism type.

TABLE 3. NUMERICAL VALUES OF THE INPUT PARAMETERS EMPLOYED FOR MODEL VERIFICATION WITH EXPERIMENTAL DATA (YANKEL, 1972) (MCCARTHY ET AL., 1976) IN FIGURE 7. PARTICULATE: DOP AEROSOL. COLLECTOR: ALUMINA GRANULES.

L_{mf}	= 6.12 cm
D_R	= 5.0 cm
D_c	= 0.0175 cm
D_P	= 1.4×10^{-4} cm
ϵ_{mf}	= 0.50
ϵ_3	= 0.50
ϵ_2	= 0.50
ϵ_1	= 1.00
U_{mf}	= 1.56 cm/s
D_G	= 1.85×10^{-7} cm^2/s
ρ_P	= 0.987 g/cm^3
ϵ_D	= 8.5
Q_{AC}	= 2.65×10^{-11} C/cm^2

TABLE 4. NUMERICAL VALUES OF THE INPUT PARAMETERS EMPLOYED FOR MODEL VERIFICATION WITH EXPERIMENTAL DATA (SCOTT AND GUTHRIE, 1959) IN FIGURE 8. PARTICULATE: DOP AEROSOL. COLLECTOR: SILICA GEL.

L_{mf}	= 12.0 cm
D_R	= 5.1 cm
D_c	= 0.010 cm
D_P	= 0.87×10^{-4} cm
ϵ_{mf}	= 0.50
ϵ_3	= 0.50
ϵ_2	= 0.50
ϵ_1	= 1.00
U_{mf}	= 2.0 cm/s
D_G	= 3.05×10^{-7} cm^2/s
ρ_P	= 0.987 g/cm^3
ϵ_D	= 8.5
Q_{AC}	= 2.65×10^{-11} C/cm^2

TABLE 5. NUMERICAL VALUES OF THE INPUT PARAMETERS EMPLOYED TO CONSTRUCT FIGURE 9.

D_R	= 5.0 cm
D_c	= 0.0175 cm
ϵ_{mf}	= 0.50
ϵ_3	= 0.50
ϵ_2	= 0.50
ϵ_1	= 1.00
U_{mf}	= 1.56 cm/s
U_o	= 3.00 cm/s
ρ_p	= 0.987 g/cm^3
ϵ_D	= 8.5
Q_{AC}	= 2.65×10^{-11} C/cm^2
Case I: D_p	= 1.0×10^{-5} cm
D_G	= 6.82×10^{-6} cm^2/s
Case II: D_P	= 1.4×10^{-4} cm
D_G	= 1.85×10^{-7} cm^2/s

is due to the fact that Brownian diffusion collection efficiencies decrease with increasing superficial gas velocity and, along with gas by-passing effects, a sharp decrease results. Case II solely represents gas by-passing effects as the interception collection efficiencies are independent of superficial gas velocity. In Case III, where both interception and inertial impaction are the controlling mechanisms, gas by-passing effects are opposed by increases in inertial impaction efficiencies with increasing superficial gas velocity. Although not shown in Figure 6, induced electrostatic collection has a similar effect as Brownian diffusion collection.

Comparison with Experimental Results

Figure 7 is a comparison of the model prediction of the overall collection efficiency as a function of superficial gas velocity to that obtained experimentally by Yankel (1972) and McCarthy et al. (1976) for a particulate diameter of 1.4 microns. The controlling collection mechanisms in Figure 7 are interception and induced

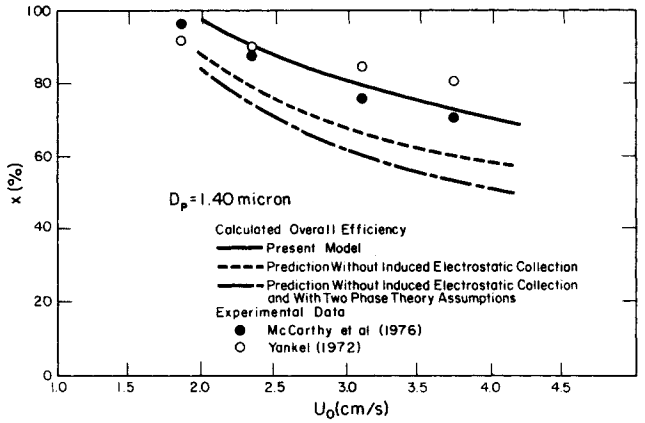

Figure 7. Comparison of the calculated values and experimental data (McCarthy et al., 1976) (Yankel, 1972) for the overall collection efficiency (%) as a function of the superficial gas velocity. The input parameters are given in Table 3.

electrostatic collection. As can be seen in Figure 7, the present model gives reasonable agreement with the experimental data. Although not shown here, a similar comparison of the predicted to experimental values (Yankel, 1972; McCarthy et al., 1976) was obtained for a particulate diameter of 0.67 microns.

Also shown in Figure 7 are some possible errors that can be introduced in the modeling of fluid bed filters. Note that poor agreement is obtained when the dielectric nature of the bed medium solids is neglected or, in addition, the two phase theory employed for estimating the superficial bubble phase gas velocity (Appendix 2). Although the importance of gas by-passing and triboelectrification effects in fluid bed filtration has been noted by other authors, (Gutfinger and Tardos, 1979; Tardos et al., 1979; Patterson and Jackson, 1977), this is the first work which enables a quantitative determination of both effects on fluid bed filtration performance. Furthermore, because the two phase theory tends to over-predict gas by-passing, apparent errors can be introduced into predicative methods. In Figure 8 the present model prediction of the overall collection efficiency is shown to compare well to the experimental data of Scott and Guthrie (1959). The controlling mechanisms in Figure 8, as in Figure 7, are interception and induced electrostatic collection. Note that introducing the same errors in Figure 8 as done previously in Figure 7 further exemplifies the importance of both collection mechanisms as well as fluidization mechanics in the modeling of fluid bed filters.

As seen in Figure 2b, when both Brownian diffusion and interception are small, a minimum in the single spherical collection efficiencies occurs. In the vicinity of the minimum, deficiencies

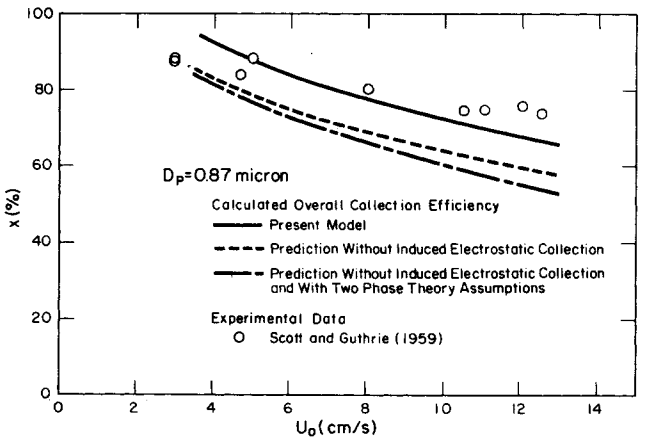

Figure 8. Comparison of the calculated values and experimental data (Scott and Guthrie, 1959) for the overall collection efficiency (%) as a function of superficial gas velocity. The input parameters are given in Table 4.

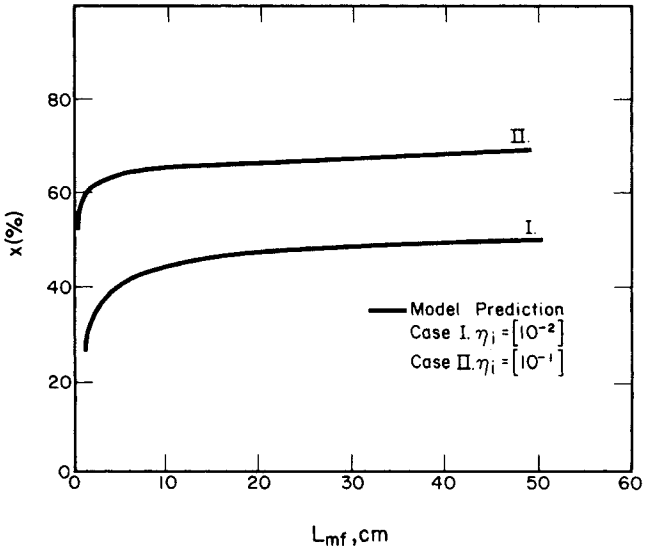

Figure 9. Dependence of the overall collection efficiency on minimum fluidization bed height. The input parameters are given in Table 5.

in the theoretical treatments to the collection mechanism problem can be seen in the works of Patterson and Jackson (1977) and Gutfinger and Tardos (1979). Furthermore, sensitivity studies show that in the vicinity of the minimum it is the collection mechanism models which tend to control the overall collection efficiency. Therefore, the present model can only be considered as an estimate to fluid bed filtration performance in this region.

EFFECT OF INITIAL BED HEIGHT AND DISTRIBUTOR TYPE

In addition to the effects of particulate diameter and superficial gas velocity, the dependence of the overall collection efficiency on the total height of the fluidized bed is important in the design of fluid bed filters. Figure 9 shows a typical simulation result obtained from the present model. It is seen in Figure 9 that increases in the overall collection efficiency become linear with increasing bed height. This is due to the fact that gas interchange rates over the added portions of the bed become increasingly smaller. Under these conditions increases in the overall collection efficiency become directly proportional to the amount of collectors added. Note from Figure 9 that the optimum bed height will, in general, be greater for smaller values of the single collector efficiencies. Also note that in the constant rate period, the model predicts that the overall collection efficiency per unit volume of bed decreases with bed height. This result is consistent with the concept of using

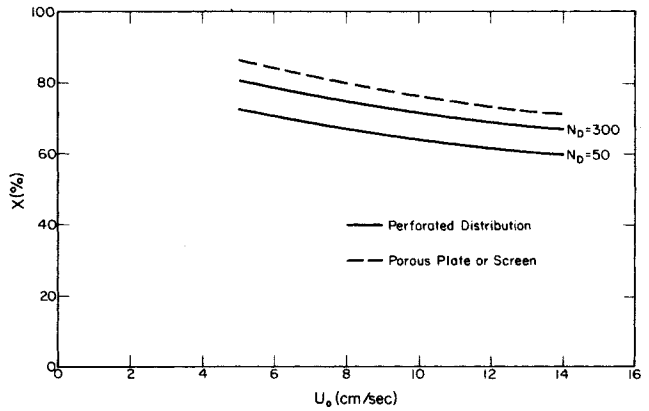

Figure 10. Dependence of the overall collection efficiency on distributor type.

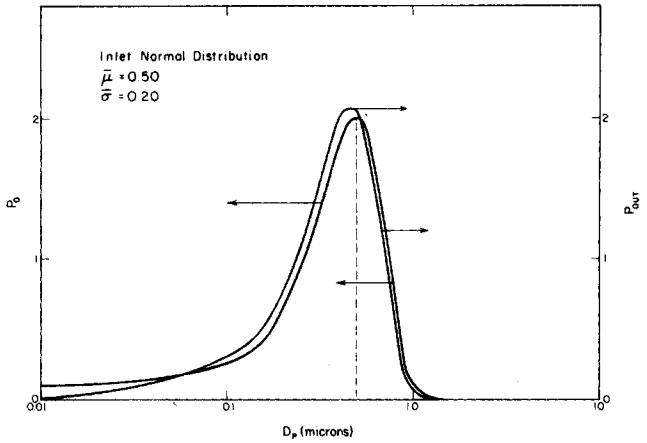

Figure 11. Quantitative behavior of particle size distribution into and out of the fluidized bed.

shallow multistage fluidized beds for achieving high collection efficiencies (Patterson and Jackson, 1977; Svrcek and Beeckmans, 1976). In order to further clarify this result, order of magnitude calculations were carried out by applying Eq. 2 near the vicinity of the distributor plate. These calculations show that typically both the gas interchange term and the rate of particulate collection term are significant near the distributor. It immediately follows that the distributor type may significantly affect the performance of fluid bed filters. Figure 10 shows a typical simulation result obtained from the present model. As can be seen, perforated distributors lead to lower overall fluid bed filtration efficiencies as compared to porous distributors or screens. Refering to Eqs. 16 and 17, perforated distributors give rise to larger initial bubble sizes than porous plates or screens. In general, larger bubbles serve to decrease gas interchange, via Eqs. 18 and 19, and to increase gas by-passing, as discussed previously, leading to somewhat lower conversions. Because of the scarcity of experimental data concerning the effects of bed height on overall fluid bed filtration performance, (Knettig and Beeckmans, 1974), the results shown in Figures 9 and 10 cannot be completely substantiated. Furthermore, it should be noted that the quality of fluidization will also affect the results shown in Figures 9 and 10.

EFFECT OF PARTICULATE SIZE DISTRIBUTION

In practical applications, the size of all particulates are distributed about some mean. Because of the fact that the overall collection efficiencies are dependent on particle size, inlet particle size distributions are generally different from those leaving. Figure 11 shows a quantitative plot of this effect predicted by the present model, where a normally distributed inlet particulate distribution results in a skewed outlet distribution. As can be seen in Figure 11, the skewed outlet distribution is due to high collection efficiencies for small diameter particulates. Outlet particulate distributions are easily calculated by multiplying the probability of occurrence of a given particle size by its corresponding penetration and normalizing the results. It should be noted that the determination of outlet particulate size distributions also has importance in the design of multistage fluid bed filters.

JETTING AT THE DISTRIBUTOR AND REGIONS OF APPLICABILITY OF THE PRESENT MODEL

Another fluidized bed collection mechanism that has appeared in the literature, in addition to those given here, is collection by jetting action at the distributor (Doganoglu et al., 1978). As far as the grid region is concerned, Rowe et al. (1979) have argued that jets are not always present in gas-solid fluidized beds, but that rapidly coalescing small bubbles may characterize this region. This observation is in conceptual agreement with the present model. Regardless of this conceptuality, it has been experimentally shown that mass and heat transfer rates in this region are much higher than in any other regions of the fluidized bed (Behie, 1972). This effect is partially accounted for in the proposed model by the inclusion of bubble size variation in the bed along with Eqs. 18 and 19. However, no accurate correlation or theory presently exists for predicting mass transfer in the grid region of a gas-solid fluidized bed.

For the systems considered here, Eq. 8 is rigorously followed indicating that reverse flow of gas in the emulsion phase can be neglected. This is consistent with the assumptions made in the model development. Furthermore, the model assumption of complete retention is ensured by comparisons of the collection efficiencies of aerosol type particulates (Doganoglu et al., 1978). The applicability limits of the present model have been explicitly given in Eq. 8 and the regions of applicability of Eq. 14. Along these lines, the present model may be somewhat improved by using more sophisticated theoretical schemes for evaluating the single collector efficiencies, e.g., Tardos et al. (1978). An alternative design approach would involve back-calculating global single collector efficiencies from the present model and bench scale fluid bed filter data. Modifications of the present model to high velocity situations, which includes flow reversal of gas as well as the effects of solids circulation, are currently underway.

NOTATION

C = Cunningham correction factor
C_{i_n} = concentration of particulate in nth compartment in phase i, g/cm^3
C_o = inlet particulate concentration, g/cm^3
C_{out} = outlet particulate concentration, g/cm^3
D_c = collector diameter, cm
D_G = molecular diffusion coefficient of particulate, cm^2/s
D_p = particulate diameter, cm
D_R = fluid bed diameter, cm
D_1 = equivalent spherical bubble diameter having the same volume as that of a bubble, cm
D_2 = equivalent spherical cloud diameter, cm
$\overline{D}_1$ = average equivalent spherical bubble diameter, cm
$\overline{D}_2$ = average equivalent spherical cloud diameter, cm
D_{1_0} = initial bubble diameter, cm
D_{1_m} = maximum bubble diameter, cm
F_{12} = gas interchange coefficient between phase 1 and phase 2 per unit volume of phase 1, 1/s
F_{23} = gas interchange coefficient between phase 2 and phase 3 per unit volume of phase 1, 1/s
G = gravitational acceleration, cm/s^2
$g(\epsilon)$ = correction factor appearing in Eq. 36
h = height from distributor plate, cm
K = dimensionless characteristic particle mobility
L = expanded bed height, cm
L_{mf} = bed height at U_{mf}, cm
N = number of bubbles in a compartment
$\overline{N}$ = average number of bubbles in a compartment
N_D = number of orifice openings on the distributor
N_I = dimensionless interception parameter, D_p/D_c
N_{Pe} = Peclet number, $U_{p_0}D_c/D_G$
P_o = probability of particulate diameter entering fluidized bed
P_{out} = probability of particulate diameter leaving fluidized bed
Q_{AC} = surface density of electric charges, C/cm^2
Q_P = charge on particulate, C
S = cross-sectional area of bed, cm^2
Stk = Stoke's number
U_i = linear velocity of gas in phase i, cm/s
$\overline{U}_1$ = average linear gas velocity in bubble phase, cm/s
U_{is} = superficial velocity of gas in phase i, cm/s
U_{3s}' = superficial velocity of gas in the emulsion phase for the slow bubble stage, cm/s
U_{mf} = minimum fluidization velocity, cm/s

U_{po} = approach velocity of particulate, cm/s
U_o = superficial gas velocity, cm/s
U_s = terminal settling velocity of particulate cm/s
V_{i_n} = volume of phase i in nth compartment, cm^3
$\overline{V}_1$ = average volume of bubble phase, cm^3
X = overall collection efficiency (%)

Greek Symbols

ϵ_D = dielectric constant of aerosol particle
ϵ_i = void fraction of gas in phase i
ϵ_{mf} = void fraction in bed at U_{mf}
ϵ_o = permittivity of free space, 8.85×10^{-21} C^2/dyne · cm^2
δ_i = volume fraction of bed occupied by phase i
$\underline{\delta}_2'$ = volume ratio between cloud and bubble phases
$\underline{\delta}_1$ = average bubble phase volume fraction
δ_2 = average cloud phase volume fraction
η_i = single spherical collector efficiency in phase i
η_{BD} = single spherical collector efficiency for Brownian motion
η_{IMP} = single spherical collector efficiency for impaction
η_{INT} = single spherical collector efficiency for interception
η_{ELECT} = single spherical collector efficiency for induced electrostatic collection
ρ_p = particulate density, g/cm^3
ρ = gas density, g/cm^3
μ = gas viscosity, g/cm · s
$\overline{\mu}$ = mean particulate diameter
$\overline{\sigma}$ = variance of particulate diameter

LITERATURE CITED

Behie, L. A., Ph.D. dissertation, "Momentum, Heat and Mass Transfer From a Grid Jet in a Large Gas Fluidized Bed," Univ. Western Ontario, Canada (1972).

Chavarie, C. and J. R. Grace, "Performance and Analysis of a Fluidized Bed Reactor. I. Visible Flow Behavior," *Ind. Eng. Chem. Fundamentals*, **14,** 75 (1975).

Chen, C. Y., "Filtration of Aerosols by Fibrous Media," *Chem. Rev.*, **55,** 595 (1955).

Ciborows, J., and L. Zakowski, "Dust Removal in a Fluidized Bed. II. Electrostatic Effects in a Fluidized Bed and their Effect on Dust-Removal Process Efficiency," *Int. Chem. Eng.*, **17,** 538 (1977).

Ciborovsky, J., and A. Wlodarsky, "On Electrostatic Effects in Fluidized Beds," *Chem. Eng. Sci.*, **17,** 23 (1962).

Davidson, J. F., and D. Harrison, *Fluidized Particles*, Cambridge Univ. Press, England (1963).

Doganoglu, Y., V. Jog, D. V. Thambimuthu, and R. Clift, "Removal of Fine Particulates from Gases in Fluidized Beds," *Trans. Inst. Chem. Eng.*, **56,** 239 (1978).

Fan, L-S. and L. T. Fan, "Transient and Steady State Characteristics of a Gaseous Reactant in Catalytic Fluidized-Bed Reactors," *AIChE J.*, **26,** 139 (1980).

Friedlander, S. K., "Mass and Heat Transfer to Single Spheres and Cylinders at Low Reynolds Numbers," *AIChE J.*, **3,** 43 (1957).

Fuchs, N. A., *The Mechanics of Aerosols*, Pergamon Press, New York (1964).

Grace, J. R., and D. Harrison, "The Behavior of Freely Bubbling Fluidized Beds," *Chem. Eng. Sci.*, **24,** 497 (1969).

Gutfinger, C., and G. Tardos, "Theoretical and Experimental Investigation on Granular Bed Dust Filters," *Atm. Env.*, **13,** 853 (1979).

Kato, K., and C. Y. Wen, "Bubble Assemblage Model for Fluidized Bed Catalytic Reactors," *Chem. Eng. Sci.*, **24,** 1351 (1969).

Knettig, P., and J. M. Beeckmans, "Capture of Monodispersed Aerosol Particles in a Fixed and in a Fluidized Bed," *Can. J. Chem. Eng.*, **52,** 703 (1974).

Kramer, H. F., and H. F. Johnstone, "Collection of Aerosol Particles in Presence of Electrostatic Fields," *Ind. Eng. Chem.*, **47,** 2426 (1955).

Kunii, D., and O. Levenspiel, "Bubbling Bed Model. Model for Flow of Gas through a Fluidized Bed," *Ind. Eng. Chem. Fundamentals*, **7,** 446 (1968).

Langmuir, I., "The Production of Rain by a Chain Reaction in Cumulus Clouds at Temperatures above Freezing," *J. Meterology*, **5,** 175 (1948).

Levich, V. G., *Physiochemical Hydrodynamics*, Prentice-Hall, Englewood Cliffs, NJ (1962).

McCarthy, D., A. J. Yankel, R. G. Patterson, and M. L. Jackson, "Multistage Fluidized Bed Collection of Aerosols," *Ind. Eng. Chem. Process Des. Dev.*, **15,** 266 (1976).

Mori, S., and C. Y. Wen, "Estimation of Bubble Diameter in Gaseous Fluidized Beds," *AIChE J.*, **21,** 109 (1975).

Nielsen, K. A., and J. C. Hill, "Collection of Inertialess Particles on Spheres with Electrical Forces," *Ind. Eng. Chem. Fundamentals*, **15,** 149 (1976).

Patterson, R. G., and M. L. Jackson, "Shallow Multistage Fluidized Beds for Particle Collection," *AIChE Symp. Ser.*, No. 161, **73,** 64 (1977).

Paretsky, L., L. Theodore, R. Pfeffer, and M. Squires, "Panel Bed Filters for Simultaneous Removal of Fly Ash and Sulfur Dioxide: II. Filtration of dilute Aerosols by Sand Beds," *J. Air Pollution Cont. Ass.*, **21,** 204 (1971).

Peters, M. H., M. S. ChE. Thesis, "Simulation of Particulate Removal in Gas-Solid Fluidized Beds Using a Modified Three Phase Bubble Assemblage Model," The Ohio State University, Columbus, OH (1979).

Peters, M. H., T. L. Sweeney, and L-S. Fan, "Reactant Dynamics in Catalytic Fluidized Bed Reactors with Flow Reversal of Gas in the Emulsion Phase," AIChE Meeting, Chicago, IL (1980).

Ranz, W. E., and J. B. Wong, "Impaction of Dust and Smoke Particles," *Ind. Eng. Chem.*, **44,** 1371 (1952).

Rowe, P. N.,and C. R. X. Yacono, "The Bubbling Behavior of Fine Powders When Fluidized," *Chem. Eng. Sci.*, **31,** 1179 (1976).

Rowe, P. N., H. J. Macgillivray, and D. J. Chessman, "Gas Discharge from an Orifice into a Gas Fluidized Bed," *Trans. Inst. Chem. Eng.*, **57,** 194 (1979).

Scott, D. S. and D. A. Guthrie, "Removal of a Mist in a Fluidized Bed," *Can. J. Chem. Eng.*, October, 201 (1959).

Svrcek, W. Y., and J. M. Beeckmans, "Kraft Furnace Effluent Gas Particulate Capture in a Multi-Plate Fluidized Bed," TAPPI., **59,** 79 (1976).

Tardos, G. I., C. Gutfinger, and N. Abuaf, "Deposition of Dust Particles in a Fluidized Bed Filter," *Israel J. Tech.*, **12,** 184 (1974).

Tardos, G. I., C. Gutfinger, and N. Abuaf, "High Peclet Number Mass Transfer to a Sphere in a Fixed or Fluidized Bed," *AIChE J.*, **22,** 1147 (1976).

Tardos, G. I., C. Gutfinger, and R. Pfeffer, "Triboelectric Effects in Filtration of Small Dust Particles in a Granular Bed," *Ind. Eng. Chem. Fundamentals*, **18,** 433 (1979).

Werther, J., "Influence of the Bed Diameter on the Hydrodynamics of Gas Fluidized Beds," *AIChE Symp. Ser.*, No. 141, **70,** 53 (1974).

Xavier, A. M., D. A. Lewis, and J. F. Davidson, "The Expansion of Bubbling Fluidized Beds," *Trans. Inst. Chem. Eng.*, **56,** 274 (1978).

Yankel, A. J., M.S. ChE. Thesis, "Fine Particle Collection With a Fixed-Fluidized Bed," University of Idaho, Moscow, Idaho (1972).

Zahedi, K., and J. R. Melcher, "Electrofluidized Beds in the Filtration of a Submicron Aerosol," *J. Air Pollution Cont. Ass.*, **26,** 345 (1976).

Zahedi, K., and J. R. Melcher, "Collection of Submicron Particles in Bubbling Electro-Fluidized Beds," *Ind. Eng. Chem. Fundamentals*, **16,** 248 (1977).

ACKNOWLEDGMENT

M. H. P. would like to acknowledge his wife, Carolyn Peters, for the typing of the manuscript. L. S. F. acknowledges the support of the Program for Energy Research, Education, and Public Service of The Ohio State University.

APPENDIX 1: SLOW BUBBLE STAGE

Equation 2 is applicable if we let $i = 1$ for the bubble phase, $i = 3$ for the emulsion phase, and $i \neq 2$. Figure A1 shows the compartments representation for a "slow bubble," cloudless stage leading up to a "fast bubble" stage with clouds. The superficial gas velocity in the emulsion phase for the slow bubble stage may be expressed from Eq. 4 as:

$$U_{3s}' = U_o - U_{1s}$$

where U_{1s} is given by Eq. 5. Gas interchange for this region is taken to be solely that between bubble and cloud phases, i.e., Eq. 18. The inlet gas to the cloud phase in the first compartment where it forms is obtained as:

$$C_{2_{n-1}} = C_{3_{n-1}}.$$

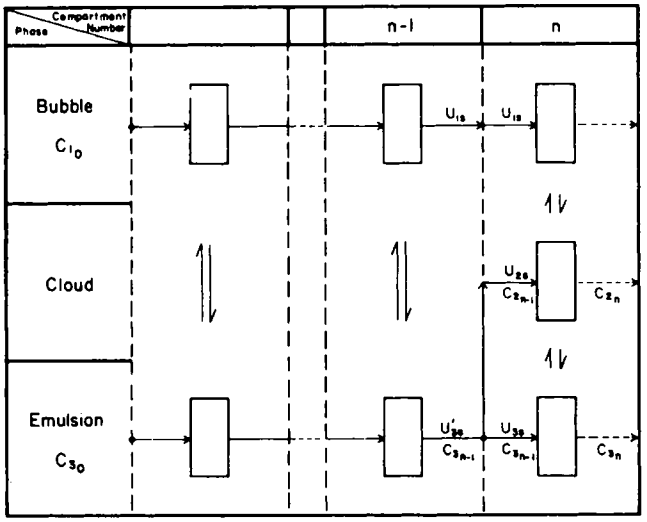

Figure A1. Compartments representation of slow bubble stage.

The volumes occupied by the bubble and emulsion phases in the nth compartment may be obtained from a straightforward simplification of Eqs. 22 and 26–29 as:

$$N = \frac{6S(\epsilon - \epsilon_{mf})}{\pi {D_{1_n}}^2 (1 - \epsilon_{mf})}$$

$$V_{1_n} = N(1/6)\pi {D_{1_n}}^3$$

$$V_{3_n} = SD_{1_n} - V_{1_n}$$

APPENDIX 2: TWO PHASE THEORY FOR ESTIMATING SUPERFICIAL GAS VELOCITIES

Determination of the superficial gas velocities in each phase is the same here as that presented by Fan and Fan (1980),

$$U_{1s} = U_o - U_{mf}$$

$$\bar{\delta}_1 = \frac{U_{1s}}{\overline{U}_1 \epsilon_1}$$

$$\bar{\delta}_2' = \frac{3U_{mf}}{\epsilon_{mf}\overline{U}_1 - U_{mf}}$$

$$\bar{\delta}_2 = \bar{\delta}_2' \bar{\delta}_1$$

$$U_{2s} = \frac{\bar{\delta}_2}{\bar{\delta}_1} \frac{\epsilon_2}{\epsilon_1} U_{1s}$$

$$U_{3s} = U_{mf} - U_{2s}$$

and $\overline{U}_1$ is computed from Eq. 10. Note that under these assumptions it necessarily follows that $Y = 1$ in Eq. 20.

Manuscript received September 18, 1980; revision received January 23, and accepted February 10, 1981.

An Approximate Mathematical Model for Three-Phase Multistaged Separators

An approximate method is developed for the simulation of three-phase, multistaged multicomponent separators in which one of the two liquid phases can be regarded as being constituted of almost one component only.

Comparisons with the complete three-phase model shows a large reduction of the required computation time and a satisfactory agreement of the obtained results.

G. BUZZI FERRARIS and M. MORBIDELLI

Istituto di Chimica Industriale
Politecnico di Milano
20133 Milano, Italy

SCOPE

Multistaged, multicomponent separators in which three phases coexist are present in many industrial processes. The mathematical model of these units consists on a large algebraic system of non linear equations, and therefore all the numerical methods proposed so far in the literature for their solution require a relatively large amount of computation time (Block and Hegner, 1976; Buzzi Ferraris and Morbidelli, 1981).

This work aims at providing a simplified approach to this problem so as to solve it more efficiently, even if approximately. In fact, in many cases of import, when the liquid phase separation occurs, each component is soluble almost only in one of the two immixible liquid phases. This is the case, for example, of many organic aqueous solutions, in which two liquid phases can coexist: an organic phase, in which all the components are present, and an aqueous phase in which all the organic components are slightly soluble. In these cases it is possible to consider the aqueous liquid phase as constituted of pure water. This

Correspondence concerning this paper should be addressed to G. Buzzi Ferraris. M. Morbidelli is with Ist. di Chimica Fisica, Politecnico di Milano, Italy.
0001-1541-82-5124-0049-$2.00